

## Supplementary Information

### Hydrogel oxygen reservoirs increase functional integration of neural stem cell grafts by meeting metabolic demands

Y. Wang<sup>1,2,3</sup>, E. R. Zoneff<sup>1,3</sup>, J.W. Thomas<sup>1</sup>, N. Hong<sup>4</sup>, L. L. Tan<sup>4</sup>, D. J. McGillivray<sup>5</sup>, A. W. Perriman<sup>6</sup>, K. C. L. Law<sup>7</sup>, L. H. Thompson<sup>7</sup>, N. Moriarty<sup>7</sup>, C.L. Parish<sup>7</sup>, R.J. Williams<sup>8</sup>, C.J. Jackson<sup>4,9,10</sup>, D.R. Nisbet<sup>1,2,3</sup>

<sup>1</sup>Laboratory of Advanced Biomaterials, Research School of Electrical, Energy and Materials Engineering, Australian National University, Canberra, ACT 2601, Australia

<sup>2</sup>The Graeme Clark Institute, The University of Melbourne, Parkville, VIC 3010, Australia

<sup>3</sup>Department of Biomedical Engineering, Faculty of Engineering and Information Technology, The University of Melbourne, Carlton, VIC 3053, Australia.

<sup>4</sup>Research School of Chemistry, Australian National University, Canberra, ACT 2601, Australia

<sup>5</sup>School of Chemical Sciences, University of Auckland, Private Bag 92019, Auckland 1142, New Zealand.

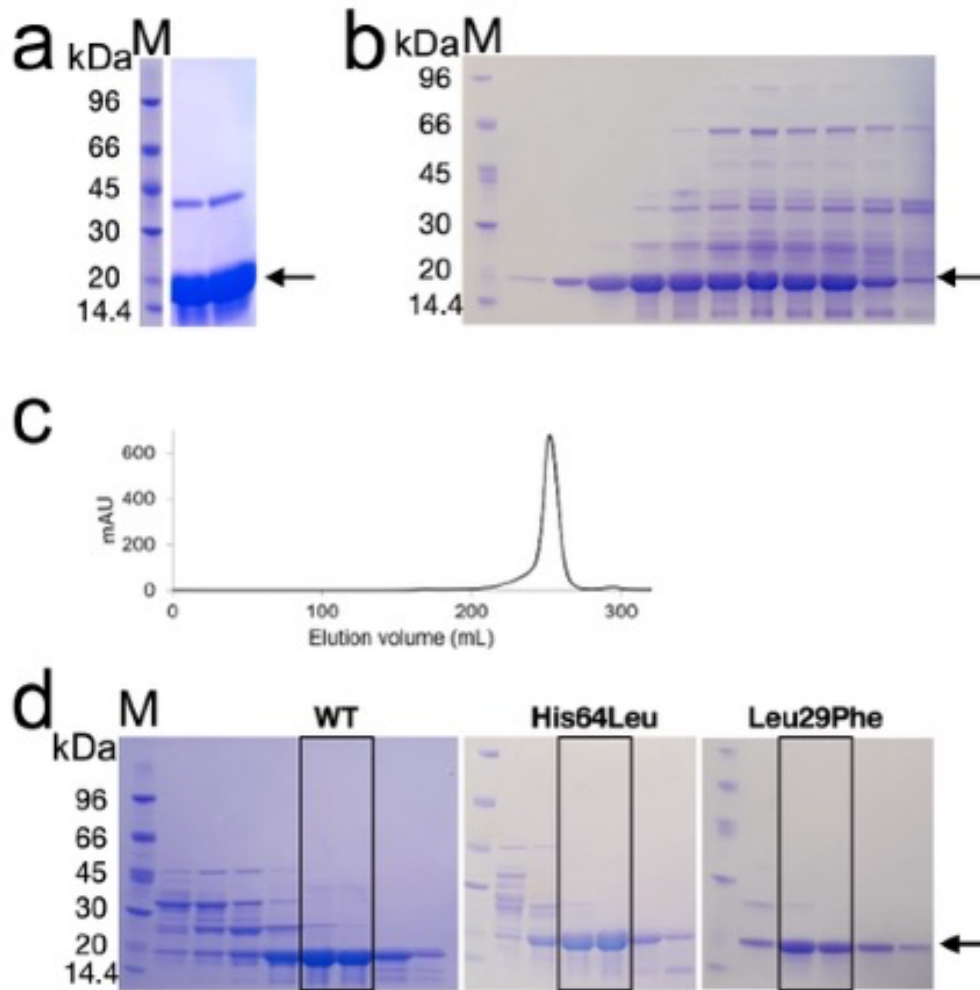
<sup>6</sup>School of Cellular and Molecular Medicine, University of Bristol, Bristol, Bristol BS8 1TD UK

<sup>7</sup>The Florey Institute of Neuroscience and Mental Health, The University of Melbourne, Parkville, VIC, Australia, 3052

<sup>8</sup>Institute for Mental and Physical Health and Clinical Translation, School of Medicine, Deakin University, Warun Ponds, VIC 3216, Australia

<sup>9</sup>Australian Research Council Centre of Excellence for Innovations in Peptide and Protein Science, Australian National University, Canberra, ACT 2601, Australia.

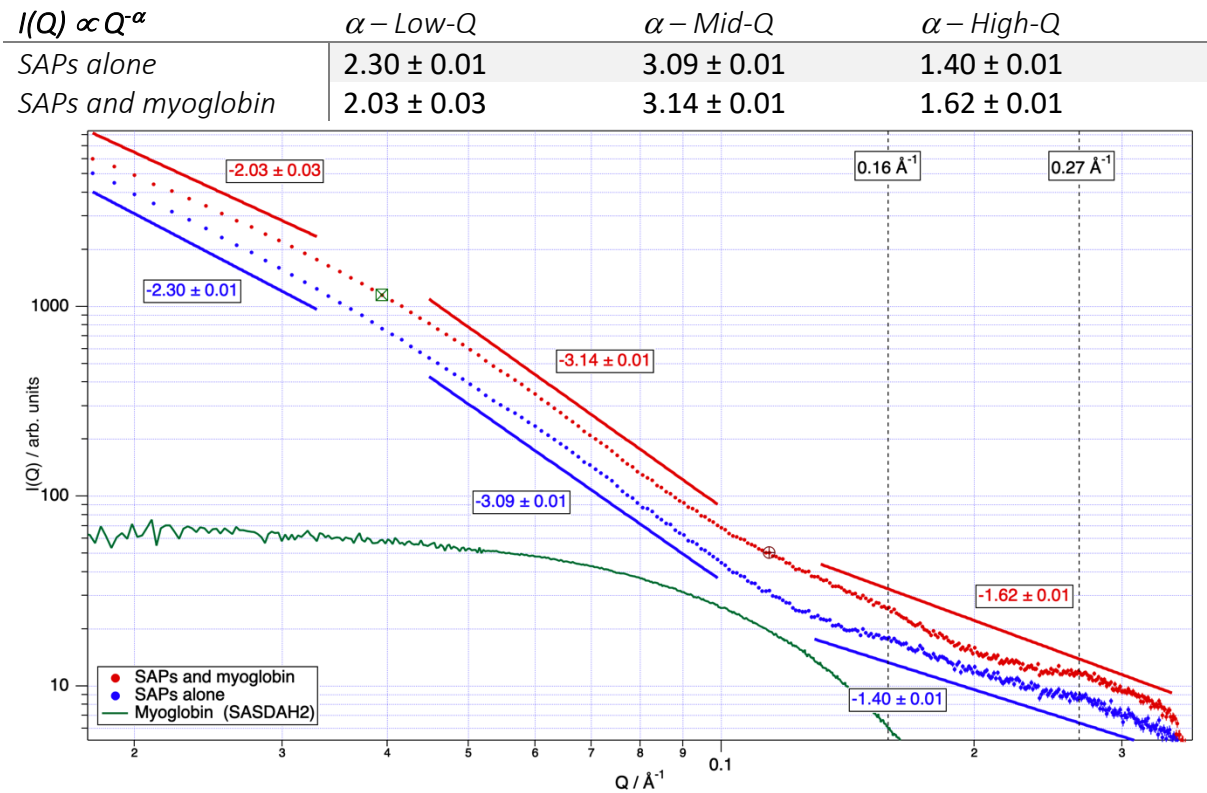
<sup>10</sup>Australian Research Council Centre of Excellence in Synthetic Biology, Australian National University, Canberra, ACT 2601, Australia.



**Supplementary Figure 1: Representative data for myoglobin purification.** **a** SDS-PAGE of commercial *Equus caballus* myoglobin after size exclusion chromatography, a dominant band (>95%) at the correct molecular weight (~17 kDa) is visible as well as a minor band that corresponds to a small amount of dimer (~34 kDa). **b** SDS-PAGE of *Physeter macrocephalus* myoglobin after anion exchange chromatography. **c** Chromatogram of *Physeter macrocephalus* myoglobin from size exclusion. **d** SDS-PAGE of *Physeter macrocephalus* wild-type, His64Leu and Leu29Phe myoglobins after size exclusion chromatography. Pure fractions that were pooled for further use are boxed. The representative images in 1a,1b,1d show a summary of at least three independent experiments.



62



63

64

65

66

67

68

69

70

71

72

73

74

75

76

77

78

79

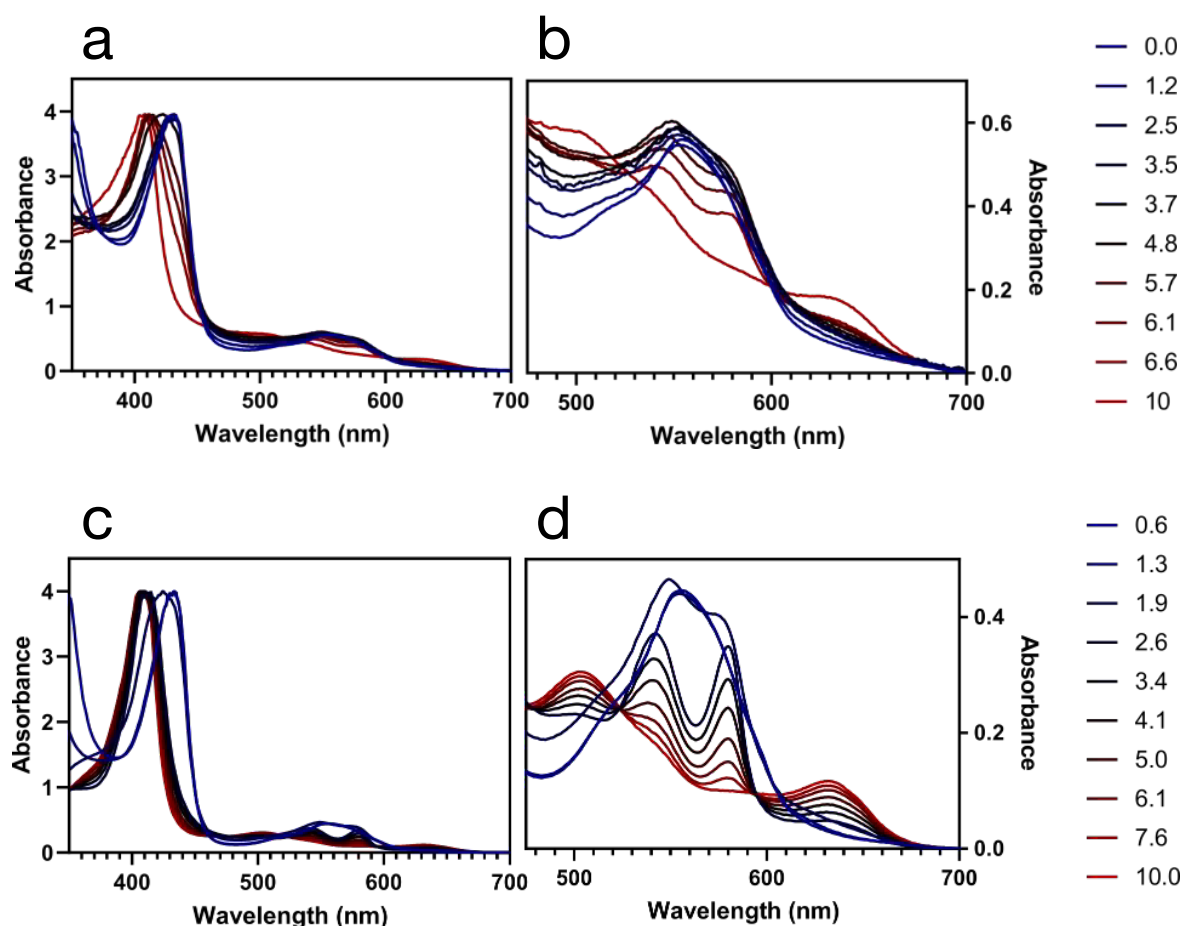
80

81

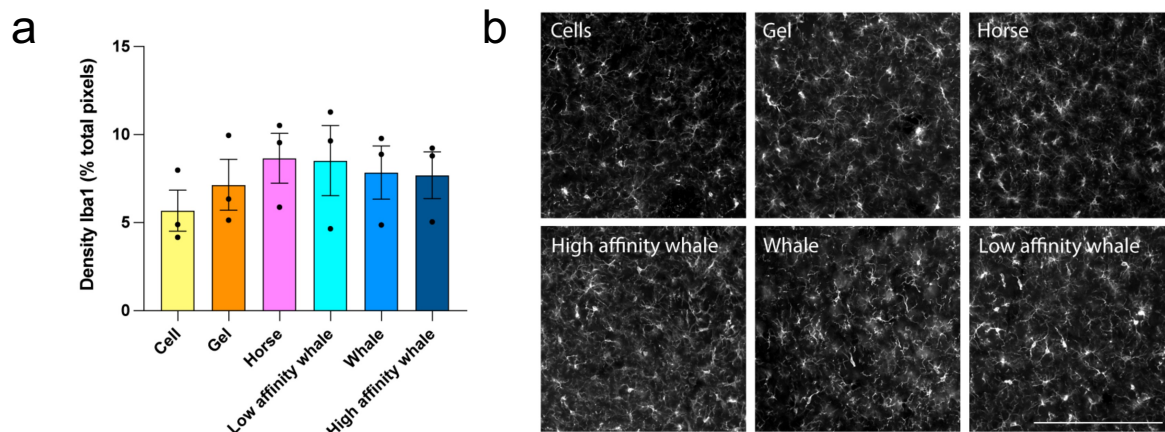
82

**Supplementary Figure 4: SAP and SAP:Horse Myoglobin SAXS analysis.** The SAP (blue) and SAP:horse myoglobin (red) samples are shown. Note that the two curves are offset for clarity. The scattering of myoglobin in solution (from the SAS database standard curve, <https://www.sasbdb.org/data/SASDAH2/>) is shown to indicate where its scattering would be significant. The scattering at low-, mid- and high-Q is shown, consistent with hydrogels and indicating random orientation of nanofibers in both samples and with minimal differences between the samples. Some weak scattering features at  $\sim 0.16 \text{ \AA}^{-1}$  and  $0.27 \text{ \AA}^{-1}$  (marked with dashed lines; real space sizes 39 Å and 23 Å respectively) are present in both samples and likely reflect cluster sizes in the hydrogels, implying that the base structure of the SAPs is unaffected by inclusion of myoglobin. A slight difference between the two samples is visible between  $0.01 \text{ \AA}^{-1} - 0.15 \text{ \AA}^{-1}$  in the SAP:Mb sample, which is consistent with scattering from the myoglobin embedded in the SAPs network. Source data are provided as a Source Data file.

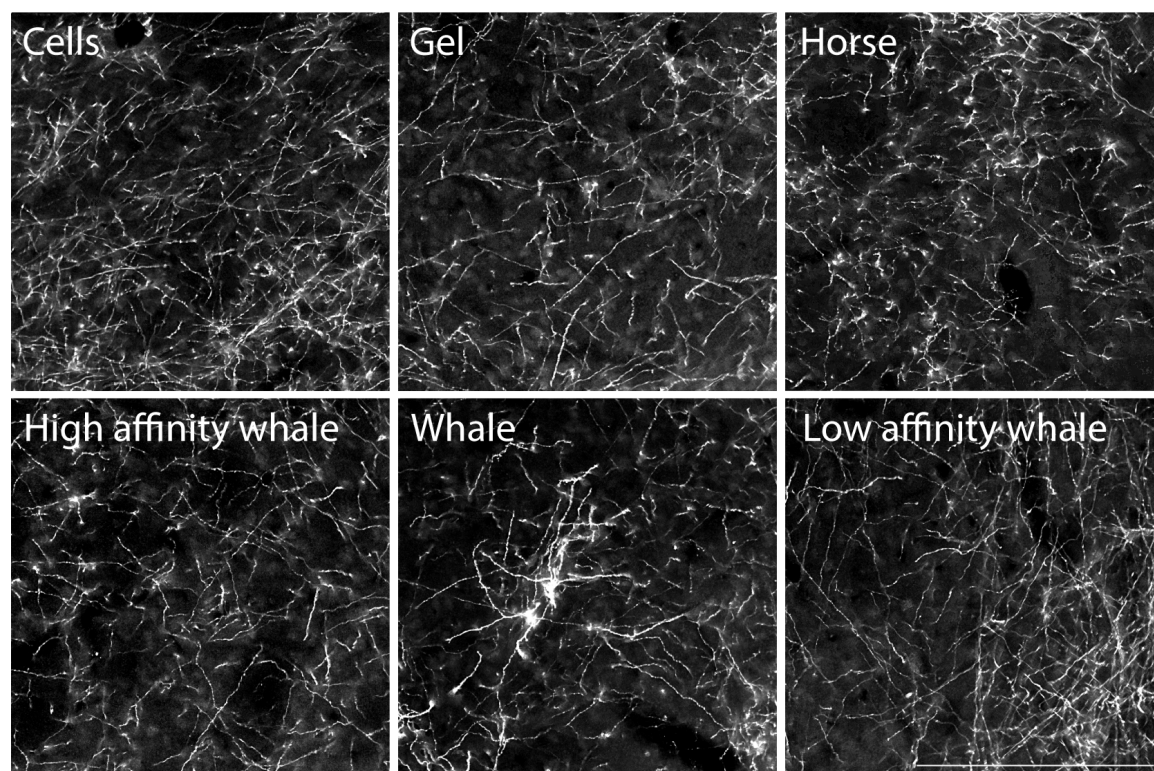




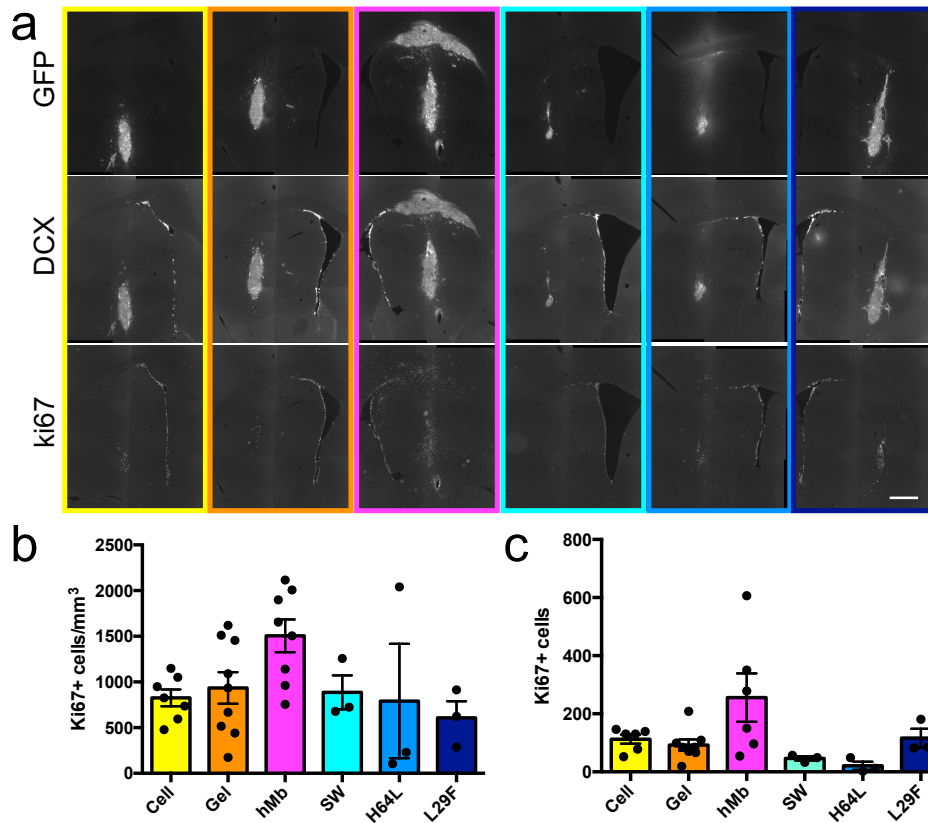
**Supplementary Figure 5: Oxidation of horse myoglobin in the presence and absence of SAP hydrogel.** **a** Functional analysis of the myoglobin:hydrogel over a 10 hour period, showing the gradual oxygenation and oxidation of myoglobin within the gel. Metmyoglobin (oxidized) is identifiable by a small peak at 628 nm, reduced absorbance between 550-600 nm, and a shift in the maximum absorbance from 426 to 409 nm. **b** Zoom on the region between 470-700 nm. **c** Functional analysis of reduced deoxymyoglobin in the absence of hydrogel over a 10 hour period, showing the formation of oxymyoglobin and oxidation of myoglobin to metmyoglobin (oxidized), which is identifiable by a small peak at 628 nm, reduced absorbance between 550-600 nm, and a shift in the maximum absorbance from 426 to 409 nm. The transition is significantly more rapid than for an the myoglobin:embedded in the SAP hydrogel. **d** Zoom on the region between 470-700 nm.



**Supplementary Figure 6: Myoglobin had no effects on the host microglia response.** **a** Density of Iba1+ microglia surrounding the GFP+ graft ( $n = 3$ ). **b** Representative images of Iba1+ immunolabeling adjacent to GFP+ graft in SAPs and SAPs+Mbs groups, respectively. Data are presented as mean  $\pm$  standard error of the mean (SEM). Scale bar represents 100  $\mu$ m. The representative images in S6b show a summary of at least three independent experiments. Source data are provided as a Source Data file.



**Supplementary Figure 7: Myoglobin-functionalised hydrogels support graft cell innervation and fibre extension.** Representative images of GFP+ fibre density within host striatum tissue. Scale bar represents 100  $\mu$ m. The representative images in S7 show a summary of at least three independent experiments.



**Supplementary Figure 8: Myoglobin has no effects on proliferation and migration.** **a** Representative images of GFP+/ DCX+/Ki67 cells in in cell only, hydrogel and Mb:hydrogel groups, respectively. Scale bar represents 500  $\mu$ m. The representative images in S8 show a summary of at least three independent experiments. **b** Density of Ki67+ proliferative cells in the graft in Cell ( $n = 7$ ), Gel ( $n = 9$ ), Horse ( $n = 8$ ), Whale ( $n=3$ ), Low affinity whale ( $n = 3$ ) and High affinity whale ( $n = 3$ ) groups. **c** Number of Ki67+ cells in graft in Cell ( $n = 6$ ), Gel ( $n = 8$ ), Horse ( $n = 6$ ), Whale ( $n = 3$ ), Low affinity whale ( $n = 3$ ) and High affinity whale ( $n = 3$ ) groups. Data are presented as mean  $\pm$  standard error of the mean (SEM). Source data are provided as a Source Data file.